Computational and Structural Biotechnology Journal 21 (2023) 3627–3638

Contents lists available at ScienceDirect

Computational and Structural Biotechnology Journal

journal homepage: www.elsevier.com/locate/csbj

Research article

Rapid microbial viability assay using scanning electron microscopy: a proof-of-concept using Phosphotungstic acid staining

Omar Zmerli [a,b,1], Sara Bellali [a,1], Gabriel Haddad [a,b,1], Akiko Hisada [c], Yusuke Ominami [d], Didier Raoult [e], Jacques Bou Khalil [a,b,*]

[a] Institut Hospitalo-Universitaire Méditerranée Infection 19-21 Boulevard Jean Moulin 13005 Marseille, France
[b] Aix-Marseille Université, Institut de Recherche pour le Développement (IRD), UMR Microbes Evolution Phylogeny and Infections (MEPHI), Marseille, France
[c] Hitachi, Ltd. Research & Development Group, 2520, Akanuma, Hatoyama, Saitama, 350- 0395, Japan
[d] Hitachi High-Tech Corporation, 882 Ichige, Hitachinaka-shi, Ibaraki-ken 312-8504, Japan
[e] Consulting Infection Marseille, Marseille, France

ARTICLE INFO

Keywords:
Scanning electron microscopy
Phosphotungstic acid
Plate count
Fluorescent microscopy
Viability

ABSTRACT

Multiple stains have been historically utilized in electron microscopy to provide proper contrast and superior image quality enabling the discovery of ultrastructures. However, the use of these stains in microbiological viability assessment has been limited. Phosphotungstic acid (PTA) staining is a common negative stain used in scanning electron microscopy (SEM). Here, we investigate the feasibility of a new SEM-PTA assay, aiming to determine both viable and dead microbes. The optimal sample preparation was established by staining bacteria with different PTA concentrations and incubation times. Once the assay conditions were set, we applied the protocol to various samples, evaluating bacterial viability under different conditions, and comparing SEM-PTA results to culture. The five minutes 10% PTA staining exhibited a strong distinction between viable micro-organisms perceived as hypo-dense, and dead micro-organisms displaying intense internal staining which was confirmed by high Tungsten (W) peak on the EDX spectra. SEM-PTA viability count after freezing, freeze-drying, or oxygen exposure, were concordant with culture. To our knowledge, this study is the first contribution towards PTA staining of live and dead bacteria. The SEM-PTA strategy demonstrated the feasibility of a rapid, cost-effective and efficient viability assay, presenting an open-view of the sample, and providing a potentially valuable tool for applications in microbiome investigations and antimicrobial susceptibility testing.

1. Introduction

Since the 20th century, electron microscopy (EM) has often been recognized as a complementary technique that provides ultrastructural information not accessible through other approaches. The key feature for producing the best micrographs was the use of staining procedures, which have a big impact on the quality and resolution of ultra structures. Staining biological samples with heavy metal salts were developed and applied with an aim of enhancing image contrast [1,2], either by staining the organism itself (positive staining) or staining the surrounding structures (negative staining). Commonly used EM stains include Phosphotungstic Acid (PTA), Ammonium Molybdate, Osmium Tetroxide, and Uranyl Acetate (UA). Among the commonly used negative stains is PTA, first used as a negative stain for EM in 1959, revealing viral ultra-structures [2]. Subsequently, several studies were conducted to explore the mechanism of interaction between PTA and different biologic samples. For bacteria, most studies describe how PTA stains polysaccharides which are usually present in the bacterial membrane and cell wall [3–5]. Since then, PTA has been a commonly used heavy metal stain, alongside other products, for microbiological EM investigations [6–8].

More recent studies using PTA in microbiological EM applications described a difference in contrast (variable electron density) visible with stained bacteria, however, this effect was interpreted as an undesired positive staining artifact [9], with few investigations done to explain the underlying mechanism for such a phenomenon. Recently, PTA was included in sample preparation protocols developed for rapid scanning electron microscopy (SEM) analyses [10–12]. Surprisingly, PTA staining

* Corresponding author at: Institut Hospitalo-Universitaire Méditerranée Infection 19-21 Boulevard Jean Moulin 13005 Marseille, France.
E-mail address: boukhaliljacques@gmail.com (J. Bou Khalil).
[1] Omar Zmerli, Sara Bellali and Gabriel Haddad contributed equally to this work and share first authorship

https://doi.org/10.1016/j.csbj.2023.07.010
Received 27 March 2023; Received in revised form 27 June 2023; Accepted 9 July 2023
Available online 11 July 2023

not only revealed bacterial ultrastructural details in diverse samples, but also revealed difference in bacterial contrast, especially when they were exposed to extreme stress conditions. Therefore, deeper investigations were necessary to explain the phenomenon of contrast variability on the micrographs of PTA-stained organisms.

Moreover, in all disciplines of microbiology, monitoring microbial viability has long been of significant interest, since it provides insight into microbial growth, survival, and metabolism [13,14]. Answering the simple question of whether the bacteria in a given sample is alive or dead remains a challenge. Several methodologies have been proposed for environmental and clinical microbiology to evaluate the viability of microorganisms in order to detect viable pathogens in food and water [15–18], or to evaluate and enhance bacterial growth under different culture conditions [19,20]. Adequately measuring microbial viability is an essential aspect in describing different microbiomes and their components. Furthermore, assessing the state of microbial viability enables researchers to investigate the efficacy of chemical, biochemical, disinfectant treatments, and antibiotics [21–25]. Although methods based on culture may require lengthy periods of time, they remain the gold standard for this type of diagnosis [26]. Other approaches have been developed based on RNA quantification [14,27], flow cytometry [18, 28], as well as specific fluorescent markers [29,30], to evaluate the viability of microorganisms. Most viability stains commonly used in flow cytometry and fluorescence microscopy, such as propidium iodide, consist of detecting the signal from damaged bacteria once the dye penetrates the cell [31]. These approaches are often more costly, thereby restricting their widespread application as part of routine microbiological examinations.

In this study, we aimed to test the hypothesis that a SEM-PTA based assay could potentially discriminate between live and dead bacteria. We investigate the viability status of microorganisms using both SEM and Energy Dispersive X-Ray (EDX) acquisitions on a selection of bacterial cultures to confirm the potential of PTA to differentially stain live and dead bacteria. We also applied the SEM-PTA assay in the evaluation of bacterial viability in a variety of settings, and conditions, comparing our results to reference culture and fluorescence methods.

2. Materials and methods

Fourteen aerobic and strict anaerobic, gram-positive and gram-negative, bacterial strains (Table 1) were selected to test the utility of Phosphotungstic acid (PTA) staining in determining bacterial viability using scanning electron microscopy (SEM).

The bacterial strains were cultured on Columbia sheep blood agar plates (BioMérieux, Marcy l'Etoile, France) at 37 °C for 24–72 h under either aerobic or anaerobic atmospheres corresponding to their growth conditions. All strains were obtained from the Collection de Souches de l'Unité des Rickettsies (CSUR, WDCM 875).

Table 1
List of bacteria tested to validate the SEM-PTA assay.

Strains tested	Gram Stain	Reference	Growth conditions
Bacillus pumilus	Gram Positive	CSUR Q0069	Aerobic
Enterococcus faecalis	Gram Positive	CSUR Q3200	Aerobic
Enterococcus faecium	Gram Positive	CSUR Q3197	Aerobic
Micrococcus luteus	Gram Positive	CSUR P9060	Aerobic
Clostridioides difficile	Gram Positive	CSUR Q8023	Anaerobic
Staphylococcus aureus	Gram Positive	CSUR Q5098	Aerobic
Cellulosimicrobium cellulans	Gram Positive	CSUR Q5038	Anaerobic
Roseomonas mucosa	Gram Negative	CSUR Q4308	Aerobic
Escherichia coli	Gram Negative	CSUR P1966	Aerobic
Serratia marcescens	Gram Negative	CSUR Q4084	Aerobic
Christensella minuta	Gram Negative	CSUR Q3516	Anaerobic
Akkermansia muciniphila	Gram Negative	CSUR P6566	Anaerobic
Acinetobacter pittii	Gram Negative	CSUR Q4392	Aerobic
Bacteroides fragilis	Gram Negative	CSUR Q3910	Anaerobic

Escherichia coli (CSUR P1966) and *Akkermansia muciniphila* (CSUR P6566) were selected as representative aerobic and strict anaerobic bacteria, respectively.

For the proof-of-concept stage, Fig. 1 shows the detailed methodology of bacterial suspension preparation followed by viability assessment using the novel SEM-PTA assay, as compared to the gold standard methods. Briefly, bacteria were suspended in Mueller Hinton Broth (MHB) medium (Sigma-Aldrich, St. Louis, MO, USA), at a concentration of 10^8~10^9 CFU/ mL, and three bacterial preparations were made: (Preparation **1**) fresh bacteria (considered mostly "live"), (Preparation **2**) dead bacteria (by heat-shock for 25 min at 90 °C), and (Preparation **3**) 1:1 mixture of live and dead bacteria. (Fig. 1**a**) Baseline viability analysis was performed on preparations (1) and (3) using validated fluorescence microscopy (FM) and plate counting techniques. Preparation (2) containing the heat-killed bacteria was inoculated on agar plates to confirm complete bacterial death. The viable plate counts were determined as previously reported (39). Briefly, serial decimal dilutions were prepared under anaerobic and aerobic conditions with Phosphate Buffered Saline (PBS) (Life Technologies, Paisley, United Kingdom), and each condition was plated in triplicate onto Columbia blood agar plates under a laminar flow cabinet and under anaerobic glove box (Don Whitley Scientific Limited, West Yorkshire, United Kingdom) with 15% CO2, 5% H2 and 80% N2 gas mixture. The agar plates were incubated 48–72 h at 37 °C. Anaerobic cultures were incubated using GasPak® anaerobic system. Overall, the survival rates were calculated as the percentage ratio of fresh culturable cell counts at time 0 and culturable cell counts after each condition. Furthermore, bacterial viability was assessed using the LIVE/DEAD BacLight kit (Invitrogen, Eugene, United States) according to the manufacturer's instructions. Briefly, 1 μL of Propidium iodide (PI) and Syto9 were added to 1 mL of bacterial suspension and incubated in the dark at room temperature for 15 min. Preparations were then cyto-centrifuged onto glass slides that were air-dried at room temperature in the dark. A grid of 3 × 3 tile images were acquired on three different regions of the slide using the confocal laser-scanning microscope (ZEISS LSM-800, Jena, Germany) with two excitation wavelengths: 483 nm for the Syto9-specific signal staining all bacteria, and 535 nm for the PI signal staining only dead bacteria. 500 bacteria per tested conditions were counted manually and clustered into green (live) and red-orange (dead) bacteria.

Then, preparations 1, 2, and 3 were made for each of the selected bacterial strains. (Table 1) Preparation (3) (½ dead, ½ live) was chosen for the validation of the SEM-PTA assay. SEM-PTA assay development consisted of identifying the optimal preparation of live and dead bacterial mixtures, followed by the optimization of PTA stain after analyzing different combinations of PTA ($PW_{12}O_{40}$) (Sigma-Aldrich, St. Louis, MO, USA) concentration and staining times. We compared fresh cultures of *Escherichia coli* and *Enterococcus faecalis* stained with 0.25%, 1%, 2% and 10% PTA (adjusted to pH 7.2 with KOH) for 60, 120, 180 and 300 s. We selected a concentration of 10% starting at two minutes, providing sufficient image contrast. We tested 10% PTA at its original pH (pH=2) and at the KOH-adjusted pH (pH=7.2); and selected the 10% PTA with pH= 7.2 for our experiment. (Supplementary Figure 1) After optimization of stain concentration and pH, the SEM-PTA assay was applied to the selected species by staining the bacterial preparations with a 10% PTA solution [3:1 (bacterial preparation: PTA)] for five minutes under agitation. The same bacterial suspensions were processed without PTA staining. Stained and not stained bacterial suspensions were then cyto-centrifuged on glass slides at 800 rpm for seven minutes and air-dried at room temperature before SEM imaging. Micrographs were recorded using Hitachi's TM4000 Plus tabletop SEM. At least ten micrographs were acquired per condition. The accelerating voltage of TM4000 Plus was at 10 kV using the BSE detector, and the magnification ranged between 2000 X and 5000 X. The function of automated imaging in the TM4000 Plus software was used, enabling fast screening of the sample, along with automated image acquisition. All acquisition settings

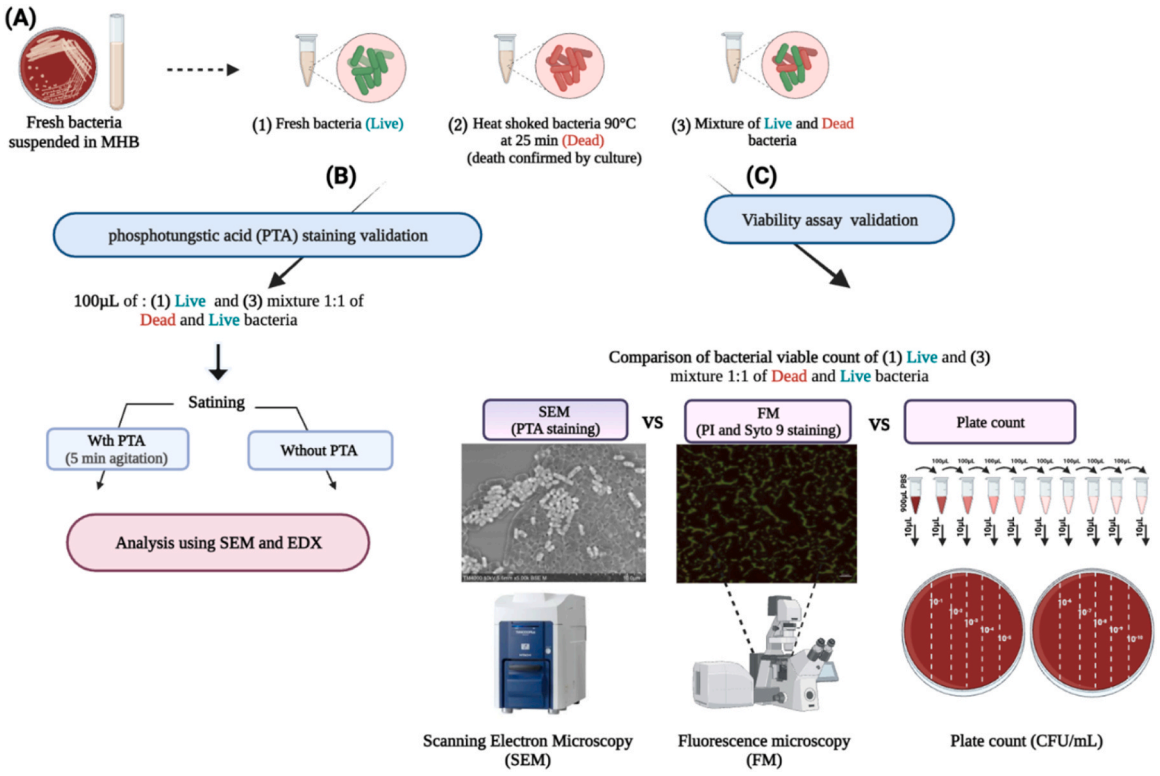

Fig. 1. Proof-of-concept workflow for bacterial viability assay using SEM and PTA.

are visible on each micrograph in the following format: Instrument, Accelerating Voltage, Working Distance, Magnification, and Detector. (Fig. 1**b**) To validate the SEM-PTA viability assay, a comparative viability analysis was done on preparations (1) and (3) to quantitatively determine bacterial viability status as compared to traditional validated viability assays. (Fig. 1**c**).

For image analysis, the procedure consisted of generating hundreds of micrographs that were randomly selected for each species. On the chosen micrographs, bacterial contrast was compared, and bacteria were clustered according to their internal contrast (bright/dark). Different morphological profiles observed on the micrographs were assigned to define the bacterial viability state. Bacterial count and line pixel profiles were performed using Fiji's Image-J software [32]. Five hundred bacteria were manually counted using the "point tool" and clustered into dark and bright bacteria for each of the tested conditions.

Following the validation of the proof of concept, expanded application steps were performed to further demonstrate the reproducibility of the observed effect. Subsequently, three extreme stress conditions were tested (exposure to oxygen, freezing and freeze-drying), in addition to different bacterial killing methods (ethanol and antibiotic exposure). The effect of oxygen exposure was tested using *A. muciniphila*, which was suspended in MHB medium and protectant medium (sucrose 10% + trehalose 5%+ antioxidants, patent number WO/2018/234645) (Table S1) under an anaerobic glove box and divided into three portions for each medium. The first portion was directly analyzed at the starting time before exposure to oxygen and the other portions were kept for one hour at room temperature under aerobic and anaerobic conditions. Bacterial viability was calculated using SEM and the viable plate count method. For the analysis of the effects of freezing and freeze-drying, *E. coli* and *A. muciniphila* were harvested from agar plates within 24 h and 48 h, respectively, and suspended into two media: (**a**) MHB medium and (**b**) protectant medium. We measured the bacterial concentration using optical Ultrospec 10 cell density meter (Biochrom, UK) and confirmed by culture (CFU method). The bacterial suspensions in each medium had an initial concentration of $\sim 10^8$ CFU/ mL for *E. coli* and $\sim 10^{10}$ CFU/ mL for *A. muciniphila* that were frozen at −80 °C for 24 h and freeze-dried as described before [33]. The bacterial viability of each condition was performed by SEM and compared to the viable plate count. For alternative bacterial killing methods analysis, *E. coli* cultures were freshly prepared and resuspended in MHB medium at a concentration of $\sim 10^7$ CFU/ mL (optical absorbance of 0.18 at a wavelength of 600 nm) measured by Ultrospec 10 cell density meter (Biochrom, UK).

Bacterial killing was performed using two strategies: ethanol and antibiotics. First, a 1:1 mixture with equal volume of 70% ethanol was prepared and incubated 30 min at room temperature. The mixture was then centrifuged and washed with MHB. One mL of the mixture was then cultured on Columbia agar + 5% sheep blood (bioMérieux, France) and incubated at 37 °C for 24 h to confirm bacterial death. Next, a mixture of preparation (1) and ethanol-killed E.coli was made. Secondly, 150 µL aliquots of the prepared cultures were distributed in three rows of a 96-well plate, with row A as control. Imipenem was chosen as an antibiotic against *E. coli*, and minimum inhibitory concentrations (MICs) of imipenem were determined using E-test and the broth microdilution method (BMD) (40). Imipenem was tested at 1x MIC and 10x MIC, according to EUCAST guidelines, in rows B and C, respectively. Sample preparation for SEM-PTA was performed as previously described (40). Micrographs of E. coli under all above conditions were then obtained at 0, 30, 60, and 120 min.

Finally, in order to evaluate the localization of the PTA stain as observed on micrographs after performing the SEM-PTA assay, fresh and heat-killed *E. coli* (CSUR P1966) suspensions were processed for EDX analysis with and without 10% PTA staining (**Sup** Fig. 2). At the start, stained and unstained bacterial suspensions were rinsed with MHB to remove the excess of PTA outside bacterial cells, then centrifuged at 3000 xg for 20 min to collect the bacterial pellet. Five microliters of the pellet were deposited on phosphorous-doped silicon (*Si*) wafers (Siltronix, France), air-dried, and analyzed using EDX (AZtecOne, Oxford Instruments, UK). The acceleration voltage was set at 15 kV, analyzing three frames at x300 magnification for each condition. EDX spectra were acquired using a mapping mode at 512 image resolution, three times

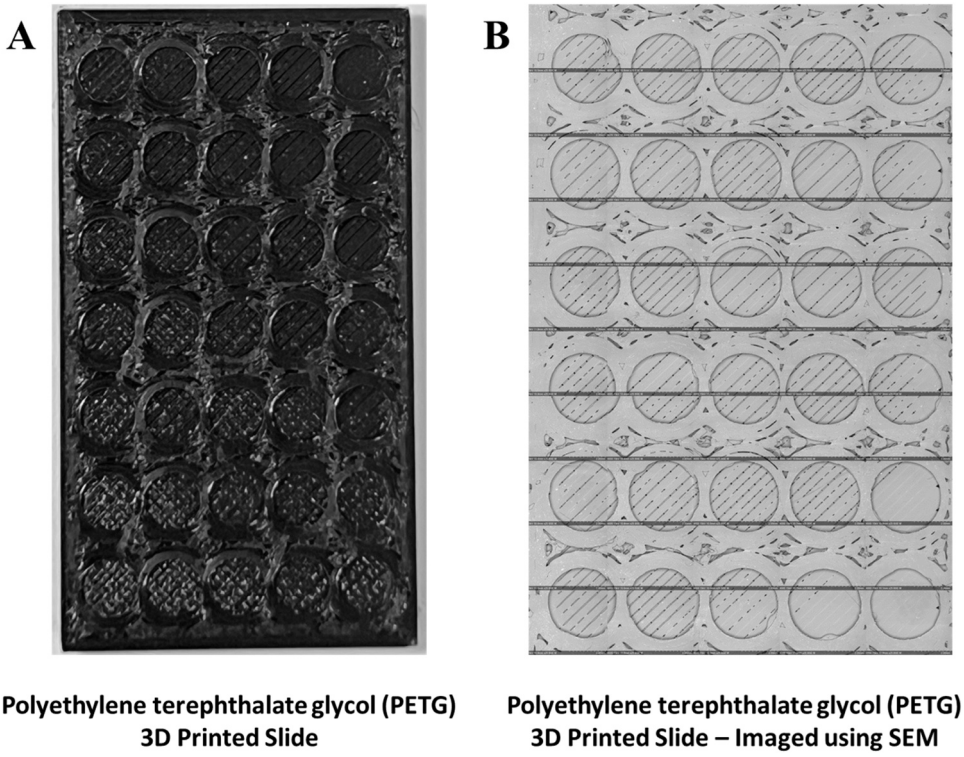

Fig. 2. A. Polyethylene terephthalate glycol (PETG) 3D printed slide developed in-house for Energy Dispersive X-Ray (EDX) analysis - eliminating the overlapping Kα peak of Silicon *Si* with the M peak for Tungsten *W*. B. Stitched images of blank slide imaged using SEM.

frame count, and 200 μs pixel dwell time. The main Kα peaks of carbon (*C*), oxygen (*O*), *Si*, tungsten (*W*), nitrogen (*N*), calcium (*Ca*), magnesium (*Mg*), sulfur (*S*), sodium (*Na*), phosphorous (*P*), chlorine (*Cl*), and potassium (*K*) were considered for this analysis. All peak values were normalized by *C*. However, due to the observed overlap of the Kα peak of Silicon *Si* with the M peak for Tungsten *W* (Supplementary Figure 2), we created a 3D-printed polyester (PETG) slide (Fig. 2) that was used for deposition of the preparation, following the same steps and parameters

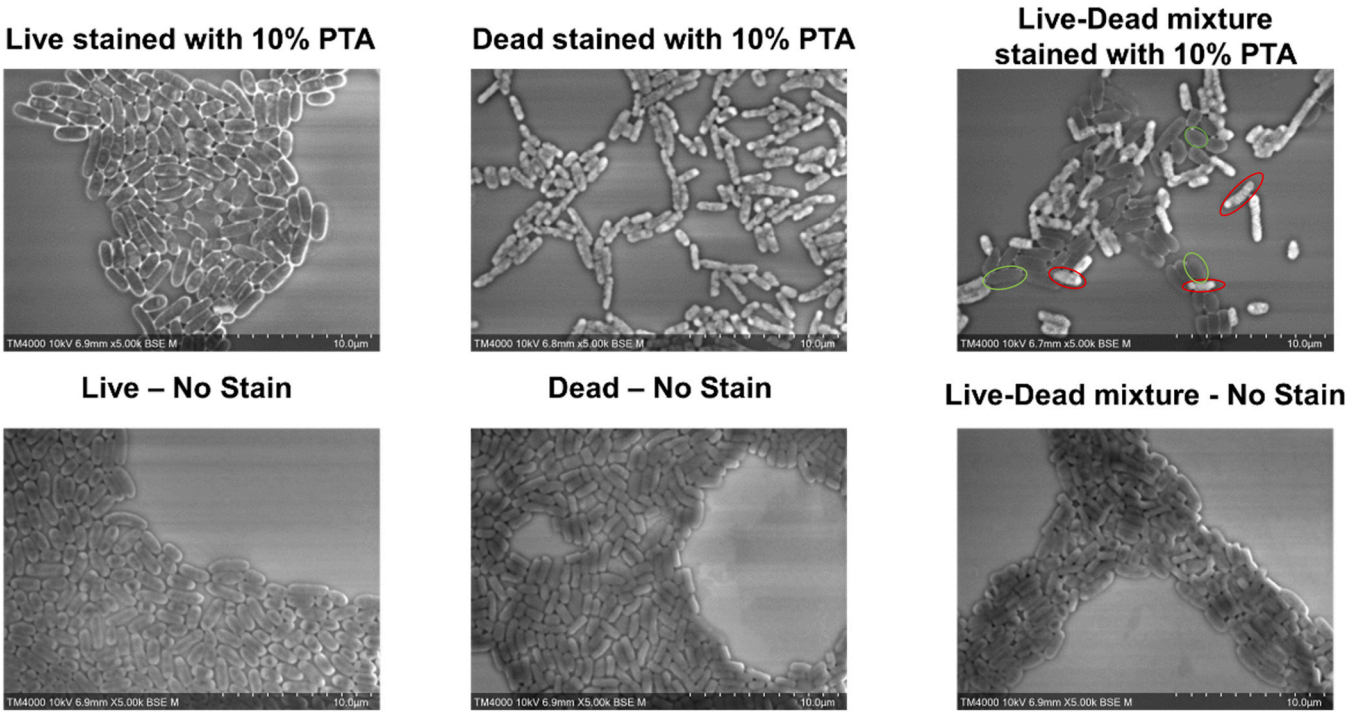

Fig. 3. Proof-of-concept on E. *coli*. Pure fresh cultures were mixed with dead bacteria (heat shocked at 90 °C) and imaged with and without PTA staining. PTA staining revealed a clear dark and bright contrast among bacteria, which was clearly absent in the unstained bacteria. Dark contrast referring to PTA localization around the live bacterial cell. (Green Circles) Bright contrast referring to PTA penetration into the dead bacterial cell. (Red Circles).

for EDX analysis, effectively eliminating the interfering *Si* peak.

The SEM-PTA viability assay patent was deposited under patent reference number 342100751 WO 01/2818 PCT.

3. Statistical analysis

The software Prism, version 5.0, was used for all statistical analyses (GraphPad Software, San Diego, CA). The viability data are provided as means standard deviations for all experiments that were performed in triplicate (SDs). We applied Kruskal-Wallis one-way analysis of variance (ANOVA) and the Mann-Whitney test (two-tailed t-test) to determine the difference between the different methods. When the *p*-value was less than 0.05, the results were considered significantly different.

4. Results

When assessing SEM micrographs of bacteria with and without PTA staining, different contrasts were detected. Without a stain, we did not observe any contrast differences between live and dead bacteria as opposed to the stained samples (Fig. 3). However, the PTA stain showed a clear and consistent difference between viable and dead bacteria. These differences were primarily evident with *E. coli* and were reproducible with the 13 other tested species, whether aerobic or anaerobic, cocci or rod shaped; shown in Supplementary Figures 3–4. On the micrographs, viable bacteria were dark centered (hypodense) with clear bright (hyperdense) edges defining the cell wall. Dead bacteria were defined as presenting an intense internal bright (hyperdense) PTA contrast, a distorted morphology and size, or complete bacterial lysis (Figs. 3–4).

In comparison to the gold standard viability assays, plate count (CFU) method revealed the viable count of *E. coli* and *Akkermansia muciniphila* in mixtures (1:1 heat-killed and fresh) to be 47.10 ± 5.89% and 46.75 ± 9.05% respectively, compared to the fresh cultures. In addition, fluorescence microscopy (FM) revealed a viability of 56.91 ± 3.93% and 59.72 ± 7.99% for *E. coli* and *A. muciniphila* in mixtures, respectively. Similarly, when using the SEM-PTA assay, *E. coli* had a viable count of 53.58 ± 7.57% and *A. muciniphila* of 50.10 ± 6.49%. At this stage, we achieved equivalent results when comparing the viability counts determined by CFU, FM, and SEM methods, with no statistically significant differences (Figs. 5 and 6). Moreover, the SEM-PTA and FM assays yielded results within one hour. While the CFU method, which is culture-based, required at least 18 h till results.

Knowing that oxygen exposure is lethal for anaerobic species, the use of a protectant medium for the conservation of these fragile organisms is necessary for sample manipulation. After demonstrating the usability of PTA in discerning live from dead organisms on SEM micrographs for both aerobic and anaerobic organisms, the assay was applied to prove the efficiency of using a protective medium and its effects on bacterial viability upon oxygen exposure. *A. muciniphila* in protectant medium enriched with antioxidants showed a comparable morphology for the fresh culture, both when exposed and when not exposed to oxygen (Fig. 7**A**). Most bacterial cells were dark centered with clear edges defining the cell wall. The viable portion of *A. muciniphila* did not significantly change after one hour of exposure (90 ± 6.00%) or non-exposure to oxygen (94 ± 2.00%) compared to the fresh culture (Fig. 7 **B- D**). These results were confirmed by the plate count method with 78 ± 1.54% cultured bacteria for exposed and 83 ± 1.35% for non-exposed bacteria (Fig. 7**D**). Nevertheless, when incubated in Mueller Hinton Broth (MHB) medium, dark *A. muciniphila* with defined edges were occasionally detected on micrographs at time 0 and after one hour under anaerobic conditions (95 ± 3.00%). Yet, after one hour of oxygen exposure, more bright bacteria with irregular morphologies were

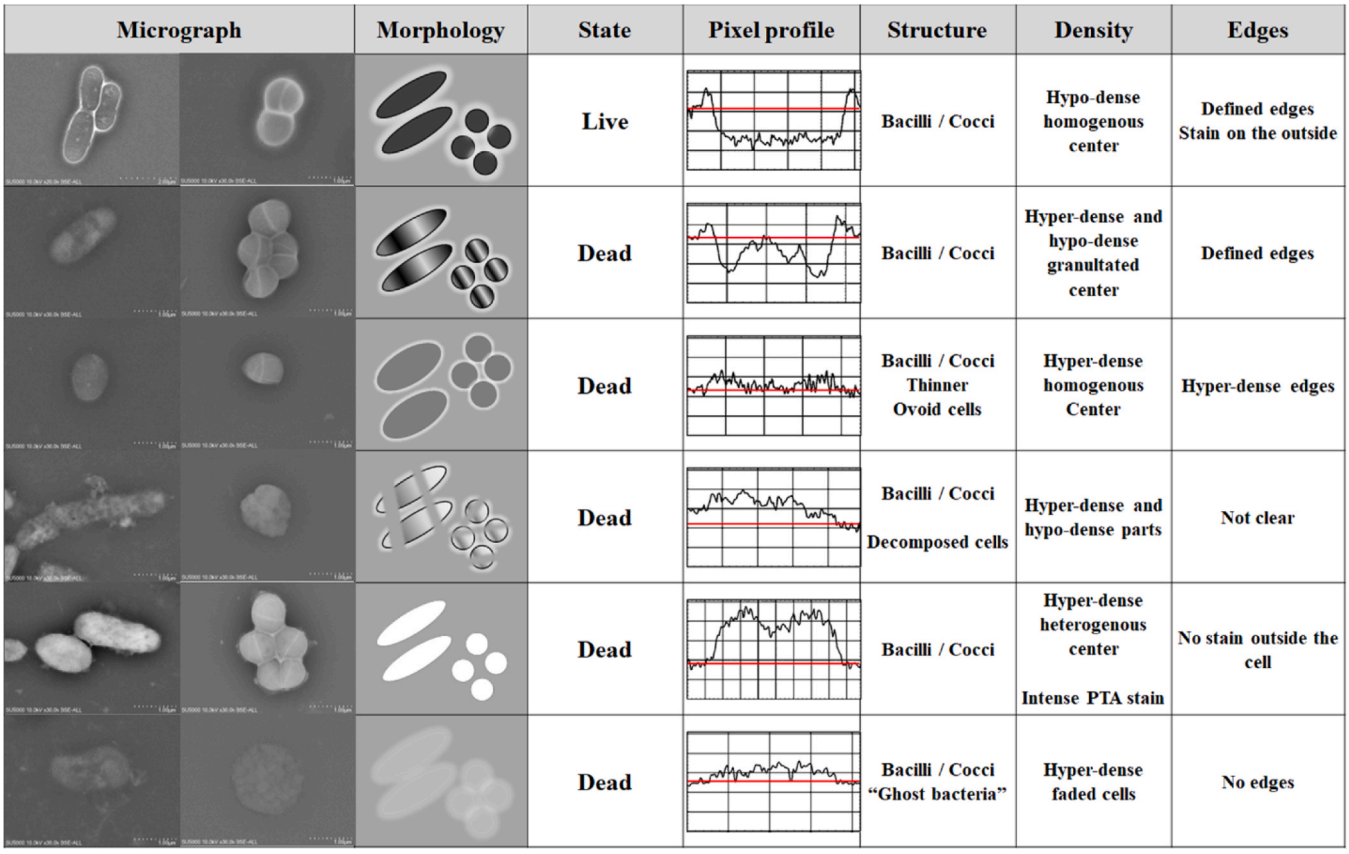

Fig. 4. Contrast analysis and different morphological profiles detected based on the internal contrast as observed on the micrographs and validated by the line pixel profile of the bacterium generated using image-J.

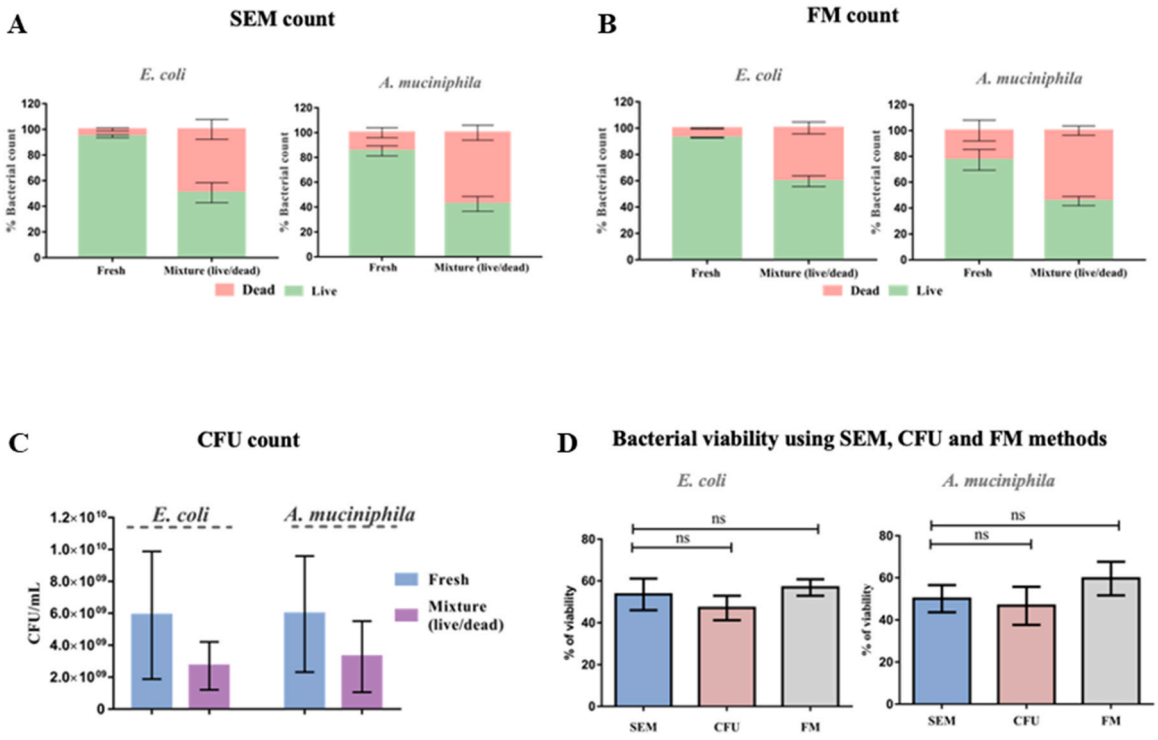

Fig. 5. Proof-of-concept by Viability Count. A. The viability count performed using scanning electron microscopy. B. The viability count performed using fluorescence microscopy. C. The viability count performed using the plate count method. D. Statistical comparison (Mann-Whitney test (two-tailed t-test)) of the bacterial viability using SEM, FM and CFU methods; demonstrating non-significant difference between the three methods. All experiments were realized in triplicate. Refer to Supplementary Figure 5 for SEM micrographs.

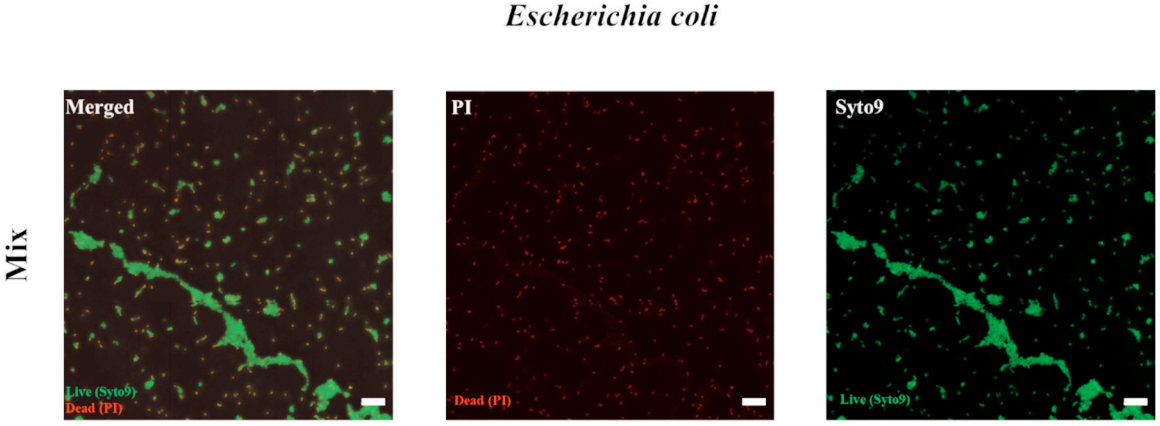

Fig. 6. *E. coli* live/dead artificial mixtures, assessed by fluorescence microscopy. Right panel: Green fluorescence for SYTO9 staining all bacteria. Middle panel: Red fluorescence for PI staining dead bacteria only. Left panel: Merged channels. Scale bars: 20 μm. Refer to Supplementary Figure 6.

present (74 ± 8.62%) (Fig. 7 **A, B and D**). After one hour of exposure, the cultured portion was lower in the absence of antioxidants (46 ± 12.38%) than in their presence (78 ± 1.54%), when compared with the SEM viable bacterial count (74 ± 8.62%, 94 ± 2.00%, respectively). Interestingly, when we compared the viability determined by SEM and CFU, we found no statistically significant differences (Fig. 7**D**).

In addition to oxygen exposure, freezing and freeze-drying are also known to have lethal effects on microorganisms. Therefore, our assay was applied to assess the viability after freezing and freeze-drying. For *A. muciniphila* and *E. coli*, few dead bacteria were detected by SEM at the starting time, on the fresh cultures in the protectant medium and MHB. The SEM viability count decreased after freezing or freeze-drying in MHB. Micrographs of both species showed a clear increase in bright bacteria (Supplementary Figure 7). Moreover, *A. muciniphila* micrographs showed bacterial inflation, and the emergence of amorphous shapes and transparent or lysed cells (Supplementary Figure 7 **B**). However, in the presence of the protectant medium, no difference in bacterial structural integrity was observed before or after freezing and freeze-drying (Supplementary Figure 7 **B**).

The SEM viability count of *A. muciniphila* and *E. coli* was compared to the CFU count in MHB and in the protectant medium. The comparison showed that counts obtained by the two methods were not statistically significant for either species (Fig. 8 **A-B**).

Furthermore, our assay was applied to determine viability following bacterial killing using ethanol and antibiotics. Micrographs obtained directly without PTA stain for ethanol killed E. *coli* showed no difference in contrast; all bacteria appearing in the same contrast (Fig. 9**).** Micrographs obtained on PTA stained fresh, ethanol killed, and live-dead

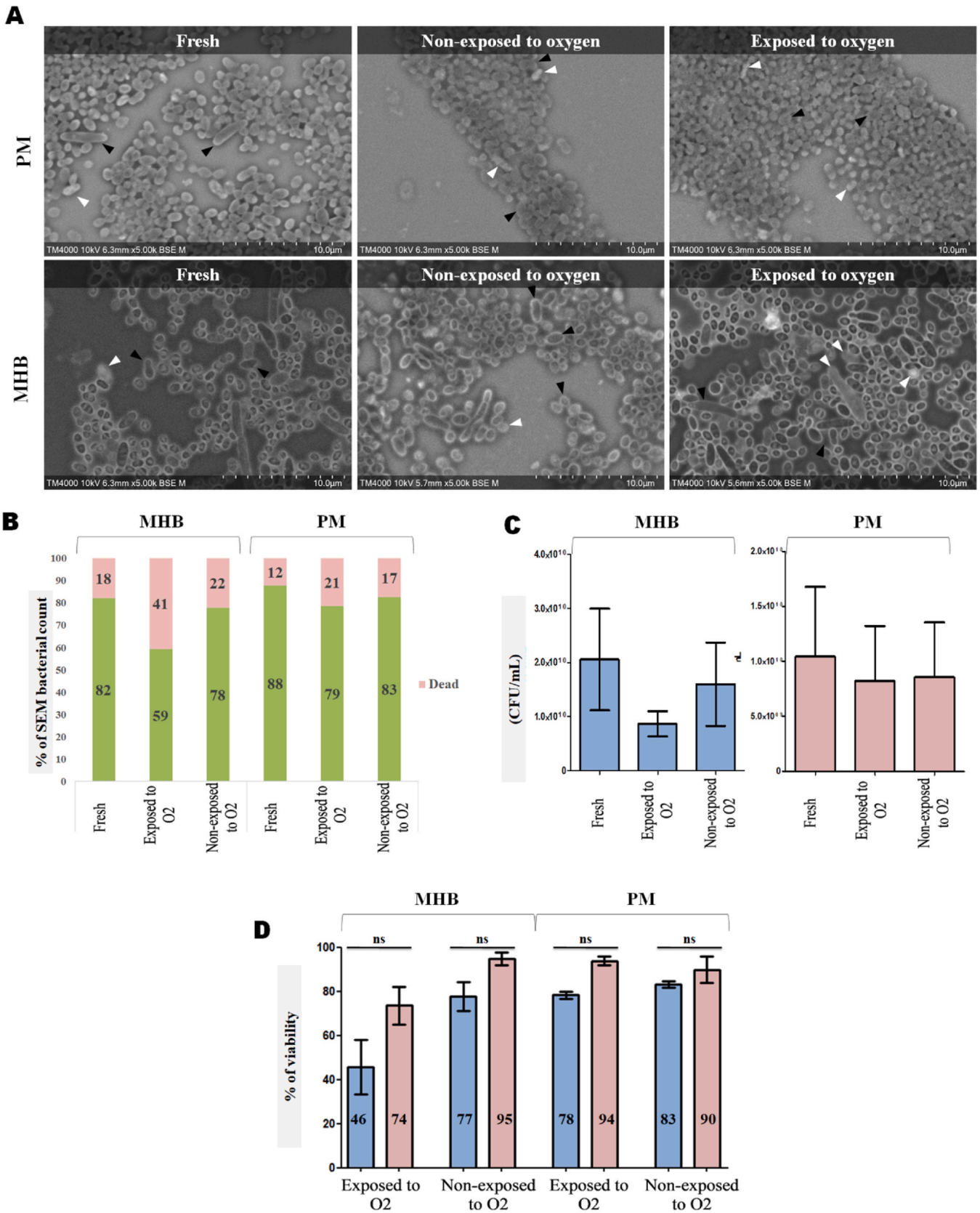

Fig. 7. A. Micrographs of PTA-stained *Akkermansia muciniphila* after one-hour non-exposure or exposure to oxygen in Mueller Hinton Broth (MHB) and in protectant medium (PM). Scale bars: 10 µm. Black arrows: live dark bacteria. White arrows: dead bright bacteria. B. The viability count performed by scanning electron microscopy. C. The viability count performed by the plate count method. D. Statistical comparison (Mann-Whitney test (two-tailed t-test)) of the bacterial viability using SEM (blue) and plate count (pink) methods. All experiments were realized in triplicate.

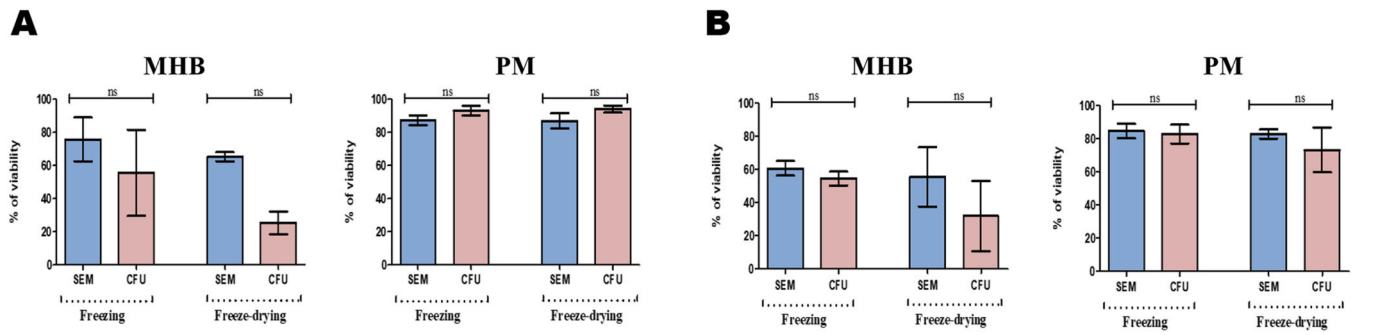

Fig. 8. A-B. Histograms comparing (Mann-Whitney test (two-tailed t-test)) SEM bacterial viability count to the plate count method in Protectant medium and MHB after freezing and freeze-drying. Experiments were realized in triplicate. Refer to Supplementary Figure 7 for SEM micrographs.

mixture of *E. coli* showed a clear difference between dead organisms that have an intense internal PTA contrast (bright) and live organisms that have a dark interior surrounded by a bright outline (Fig. 9).

Micrographs obtained successively for Imipenem-treated *E.* coli revealed evident growth of *E. coli* in the control group, with a clear dark signal (Fig. 10). Dead organisms were visible starting 15 min of incubation with 1 x MIC with the appearance of bright bacterial structures, which were considerably more numerous at 120 min (Fig. 10). The effect was more pronounced in the 10 x MIC group as a complete absence of live organisms was observed at 60 min with a total lysis and disintegration of bacteria at 120 min (Fig. 10).

EDX analysis performed for detecting the localization of the PTA stain uncovered the element Tungsten (*W*) in the stained controls without bacteria. This element was not detected in any of the non-stained live or dead bacterial spectra and was thus selected as the signature element of PTA. Surprisingly, an obvious tungsten (*W*) peak was detected only on the EDX spectra of dead stained and rinsed *Escherichia coli* and was not visible in the case of fresh stained and rinsed bacteria. EDX analysis done on PETG slides allowed the demonstration of W localization in both stained and unstained, live and dead bacteria. No significant signal was detected in unstained live and dead bacteria. A clear rim of W is observed around PTA-stained live bacteria. A strong *W* signal was evident in PTA-stained dead bacteria, overlapping with the electron dense internal staining observed on the SEM micrograph. (Fig. 11).

5. Discussion

The rapid assessment of microbial viability is of utmost importance in many fields of microbiology including the clinical, environmental, and agri-food areas. Here, we report for the first time a new rapid approach for bacterial viability testing using SEM and PTA, applicable to different type of samples. We first tested controls of live and dead bacteria, then looked at the proportion of dead bacteria in exposed to several different stressful states including exposure to oxygen (anaerobes), heat-shock, ethanol, and antibiotic. Finally, we evaluated the presence and concentration of tungsten in the living and dead bacteria by analyzing presence of Tungsten (*W*) in the bacteria. This allowed us to demonstrate that the membrane permeability to the tungsten present in PTA is related to the bright appearance of dead bacterial cells.

PTA is one of the widely used negative stains, used as a contrast agent to reveal the detailed morphology of various structures [34–37]. Despite major structural differences between viral particles and bacteria, several studies have used the PTA negative stain to gain more insights into the ultrastructural changes in bacterial cells after treatment with different agents (e.g. antimicrobial peptide temporin L, Bovine Lactoferrin etc.) [38–41]. We observed in the EM micrographs reported in these studies that the treated bacteria presented a contrast different to that of the controls. However, none of these studies reported the importance of that differential contrast in distinguishing between damaged and intact bacteria. On the contrary, such strong contrasts were considered as unwanted positive staining artifacts to be avoided in EM sample preparation protocols [6]. Mechanistically, one possible explanation for the interaction between PTA and bacteria is the formation of an electrostatic force, owing to the negatively charged bacterial membrane/cell wall due to the presence of Teichoic Acid in gram positive organisms and Lipopolysaccharide in gram negative organisms. This aligns with our observation of PTA distribution based on bacterial viability status, which affects the presence of these molecules on the bacterial surface. However, it is evident that this mechanism of PTA interaction depends on a number of chemical properties of the solution being used, including pH [42]. Some works describe the potential use of PTA in synthetic chemistry and its integration in nanoparticles, exploiting the unique chemical properties of the PTA molecule [43,44]. However, within the scope of our work, we used aqueous PTA with a neutral pH to perform a short staining step. More studies are needed to further describe the interaction of the PTA molecule with the chemical structure of bacterial membranes and internal milieu.

Moreover, the same *E. coli* and *A. muciniphila* strains tested here were analyzed in another study performed at our facility, under similar conditions using a protectant medium, and leading to similar viability results when compared to those obtained by culture and flow cytometry [10]. On the micrographs of that study, the SEM analysis was used to confirm the viability results obtained by culture and flow cytometry. We compared the morphological features and size of bacteria before and after storage, without noticing the difference of contrast [10].

In this study, we demonstrated that this intracellular contrast (positive staining) was provided from the penetration of PTA when bacteria were dead or under stress, due to membrane damage. This hypothesis was confirmed by the detection of tungsten (*W*) using SEM-EDX analysis in dead bacteria mounted on PETG slides that we designed for this particular use; proving the concept that the SEM-PTA assay could effectively discriminate between live and dead bacteria.

This new SEM-PTA assay provided results similar to those obtained by traditional plate count and FM methods. SEM-PTA also yielded results in a short time (<20 min) compared to the culture used as the gold standard, which requires long incubation times (12–72 h or days) to yield results. Furthermore, the sample preparation is rapid, straightforward, and cost-effective in terms of consumables, compared to FM, flow cytometry or molecular methods [14].

The SEM-PTA assay revealed all microorganisms and components present in the sample as well as the viability status (dead and live) of bacteria. In contrast, the plate count technique only yields information on cultured and viable bacteria. Therefore, by considering only live bacteria, SEM-PTA assay could reduce the gap between microscopic and cultured counts, also known as “the great plate count anomaly” [45]. This discrepancy can be explained by the dead bacteria included in the microscopic count. This phenomenon was recently explained in a study comparing sorted metagenomics of live and dead bacteria with microbial culturomics, where the majority of not yet cultured bacteria were

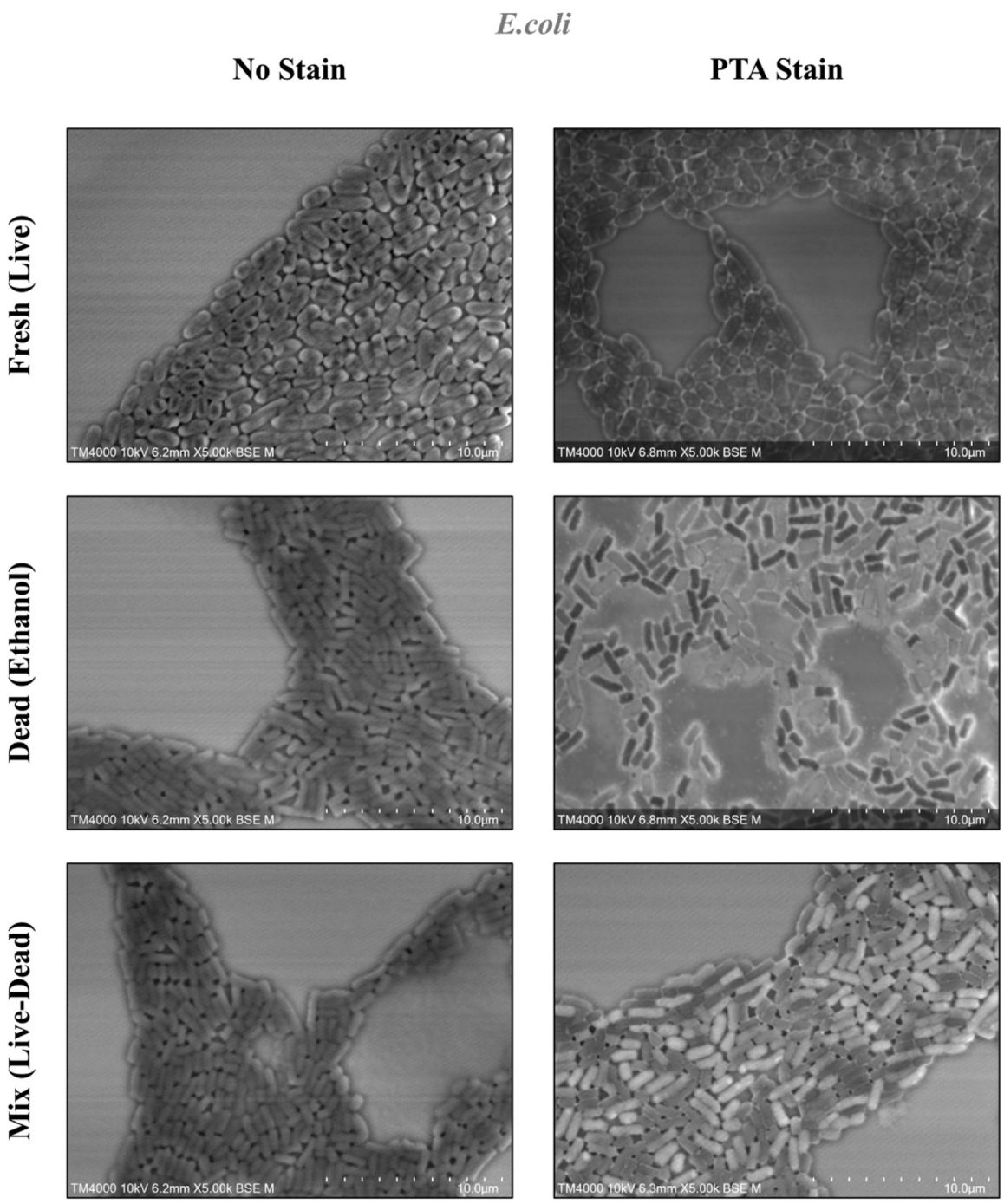

Fig. 9. SEM-PTA viability assay applied to fresh *E. coli* (upper panel), *E. coli* subjected to killing by ethanol (middle panel), and a mixture of both (lower panel). Micrographs show not stained and PTA-stained bacteria. Acquisition settings are visible on each micrograph in the following format: Instrument, Accelerating Voltage, Working Distance, Magnification, and Detector.

dead or rare [46]. Moreover, applying this assay can greatly expand researchers' ability to describe complex samples, such as those of multiple microbiomes, by providing direct access to real-time content of the sample. This might potentially help demystify the discordance observed between culturomics and metagenomics in identifying microorganisms, which is in part due to the presence of dead microorganisms that become unculturable [46,47].

The main limitation of this SEM strategy is the manual count which can be replaced by creating an automatic image analysis system for bacterial classification based on their differential contrast. Despite this limitation, SEM-PTA assays provide high resolution micrographs with a magnification high enough to reveal important ultrastructural features, along with the ease of rapidly scanning a fairly large part of the landscape. These features made SEM-PTA assays a potential candidate for the development of an automated high throughput rapid viability assessment method that can be used to quickly detect and estimate the number of viable bacteria in various samples. Once automated, this assay could easily be implemented to evaluate bacterial viability in vivo in various fresh clinical samples or even after treatment, in a short space of time. Other applications would allow researchers to monitor cultures of fastidious microorganisms in real time, or to carry out the assessment of novel antimicrobial drugs.

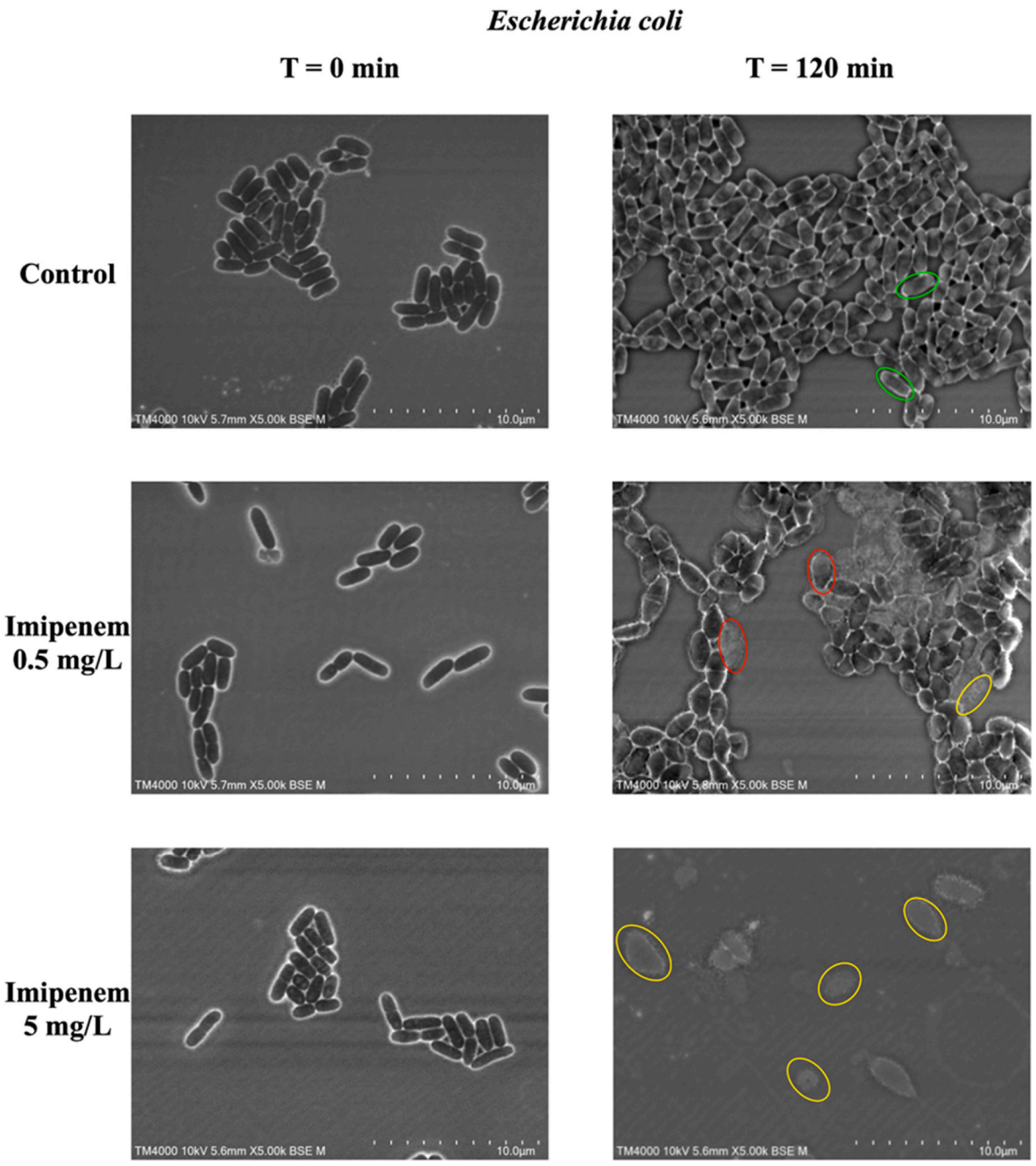

Fig. 10. SEM-PTA viability assay applied to fresh *E. coli* (upper panel), *E. coli* subjected to killing by imipenem at 0.5 mg/L (middle panel), and *E. coli* subjected to killing by imipenem at 5 mg/L (lower panel). Micrographs show PTA-stained bacteria at different time points (0 and 120 min) with clear distinction of live (green circles), dead (red circles) and total lysed/disintegrated bacteria (yellow circles). Acquisition settings are visible on each micrograph in the following format: Instrument, Accelerating Voltage, Working Distance, Magnification, and Detector. Refer to Supplementary Figure 8 for detailed SEM micrographs at all time-points.

Funding

This work was supported by a grant from the French Government managed by the National Research Agency under the "Investissements d'avenir (Investments for the Future)" program with the reference ANR-10-IAHU-03 (Méditerranée Infection), by the Région Provence-Alpes-Côte-d'Azur and the European funding FEDER PRIMI. In addition, the collaborative study conducted by IHU Méditerranée Infection and the Hitachi High-Tech Corporation is funded by the Hitachi High-Tech Corporation.

CRediT authorship contribution statement

Conceptualization, Formal analysis, Methodology, Supervision: **D.R** and **J.B.K.**; Resources, Validation: **A.H.** and **Y.O.**; Formal analysis: **S.B.**, **G.H.** and **O.Z.**; Writing – original draft: **S.B.**, **G.H.**, and **O.Z.**; Writing – review & editing: **S.B.**, **G.H.**, **O.Z.**, **J.B.K.**, and D.R. All authors have read and agreed to the published version of the manuscript.

Declaration of Competing Interest

The authors declare the following financial interests/personal relationships which may be considered as potential competing interests: Authors would like to declare that D.R. was a consultant in microbiology

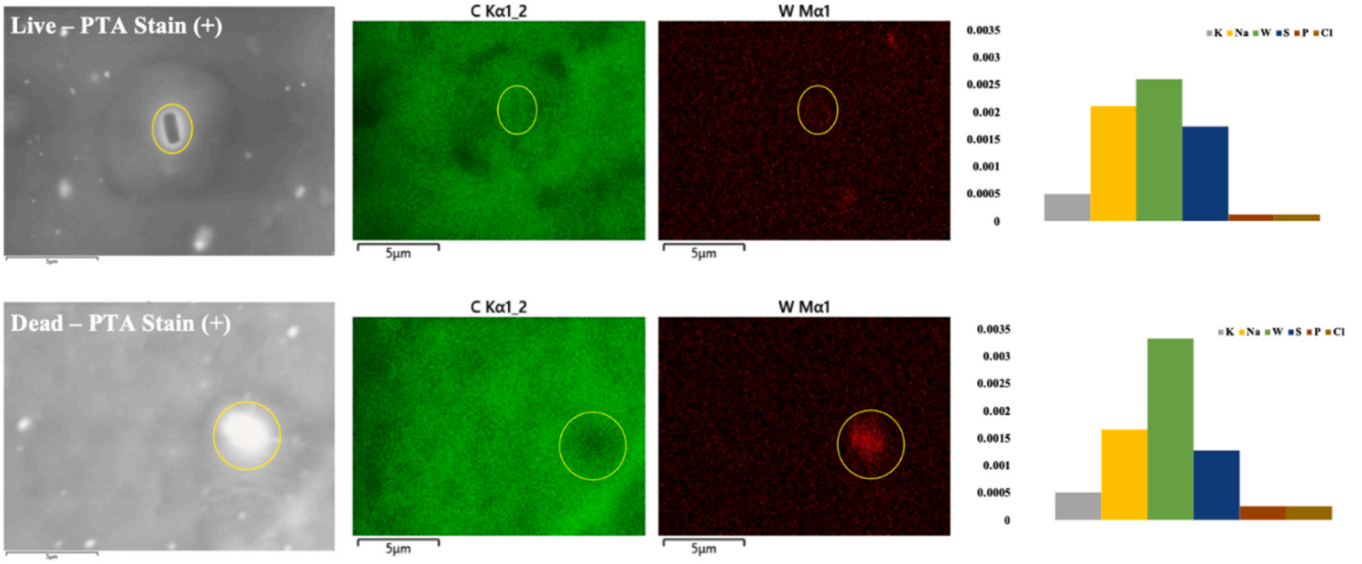

Fig. 11. Proof of PTA Stain Localization using Energy-dispersive X-ray spectroscopy analysis. EDX visual representation of PTA localization according to viability status of PTA-stained bacterial cells. Hypo-dense (dark) bacterium, considered live, shows a clear external contour signal of Tungsten, as compared to the hyper-dense (bright) bacterium, considered dead, showing a complete overlap of Tungsten and Carbon indicating the presence of tungsten within the bacterium.

for the Hitachi High-Tech Corporation from March 2018 until March 2021. Y.O. is employed by the company Hitachi High-Tech Corporation. A.H. is employed by the company Hitachi, Ltd. Personal fees of G.H., S. B., and J.B.K. are paid through a collaborative contract from the company Hitachi High-Tech Corporation. O.Z. declares no relevant competing interest. This work was supported by a grant from the French Government managed by the National Research Agency under the "Investissements d'avenir (Investments for the Future)" program with the reference ANR-10-IAHU-03 (Méditerranée Infection), by the Région Provence-Alpes-Côte-d'Azur and the European funding FEDER PRIMI. In addition, collaborative study conducted by IHU Méditerranée Infection and the Hitachi High-Tech Corporation is funded by the Hitachi High-Tech Corporation.

Data availability

All the generated data are included in the Results section and in Supplementary Material.

Acknowledgments

This work received support from Hitachi High-Tech Corporation.

Appendix A. Supporting information

Supplementary data associated with this article can be found in the online version at doi:10.1016/j.csbj.2023.07.010.

References

[1] Watson ML. Staining of tissue sections for electron microscopy with heavy metals. J Biophys Biochem Cytol 1958;4:727–30. https://doi.org/10.1083/jcb.4.6.727.
[2] Brenner S, Horne RW. A negative staining method for high resolution electron microscopy of viruses. Biochim Et Biophys Acta 1959;34:103–10. https://doi.org/10.1016/0006-3002(59)90237-9.
[3] Everett MM, Miller WA. The role of phosphotungstic and phosphomolybdic acids in connective tissue staining I. Histochemical studies. Histochem J 1974;6:25–34. https://doi.org/10.1007/BF01011535.
[4] Quintarelli G, Zito R, Cifonelli JA. On phosphotungstic acid staining. I. J Histochem Cytochem. 1971;19(11):641–7. https://doi.org/10.1177/19.11.641.
[5] Costello J, Blaize J, L'Amoreaux W, McCoy E. Ultrastructure of the pathogenic bacteria mobiluncus mulieris. MAM 2007:13. https://doi.org/10.1017/S1431927607076258.
[6] Kim K-W, Lee I-J, Hyun J-W, Lee Y-H, Park E-W. Different profiles of the negatively stained citrus canker bacterium xanthomonas citri pv. citri depending on culture media and heavy metal stains. Plant Pathol J 2010;26:90–2. https://doi.org/10.5423/PPJ.2010.26.1.090.
[7] M.A. Hayat Principles and techniques of electron microscopy: biological applications. 1989.
[8] Sahiro K, Kawato Y, Koike K, Sano T, Nakai T, Sadakane M. Preyssler-type phosphotungstate is a new family of negative-staining reagents for the TEM observation of viruses. Sci Rep 2022;12:7554. https://doi.org/10.1038/s41598-022-11405-3.
[9] Nixon HL, Harrison BD. Electron microscopic evidence on the structure of the particles of tobacco rattle Virus582. J Gen Microbiol 1959;21:582–90. https://doi.org/10.1099/00221287-21-3-582.
[10] Bellali S, Bou Khalil J, Fontanini A, Raoult D, Lagier J-C. A new protectant medium preserving bacterial viability after freeze drying. Microbiol Res 2020;236:126454. https://doi.org/10.1016/j.micres.2020.126454.
[11] Haddad G, Bellali S, Takakura T, Fontanini A, Ominami Y, Bou Khalil J, et al. Scanning electron microscope: a new potential tool to replace gram staining for microbe identification in blood cultures. Microorganisms 2021;9:1170. https://doi.org/10.3390/microorganisms9061170.
[12] Bellali S, Lo CI, Naud S, Fonkou MDM, Armstrong N, Raoult D, et al. Parabacteroides massiliensis sp. nov., a new bacterium isolated from a fresh human stool specimen. New Microbes N Infect 2019;32:100602. https://doi.org/10.1016/j.nmni.2019.100602.
[13] Barer M.R., Harwood C.R. Bacterial Viability and Culturability. Advances in Microbial Physiology, vol. 41, Elsevier; 1999, p. 93–137. https://doi.org/10.1016/S0065–2911(08)60166–6.
[14] Keer JT, Birch L. Molecular methods for the assessment of bacterial viability. J Microbiol Methods 2003;53:175–83. https://doi.org/10.1016/S0167-7012(03)00025-3.
[15] Adams BL, Bates TC, Oliver JD. Survival of *Helicobacter pylori* in a Natural Freshwater Environment. Appl Environ Microbiol 2003;69:7462–6. https://doi.org/10.1128/AEM.69.12.7462-7466.2003.
[16] Brauge T., Midelet-Bourdin G., Soumet C. Viability Detection of Foodborne Bacterial Pathogens in Food Environment by PMA-qPCR and by Microscopic Observation. In: Bridier A, editor. Foodborne Bacterial Pathogens, vol. 1918, New York, NY: Springer New York; 2019, p. 117–28. https://doi.org/10.1007/978–1-4939–9000-9_9.
[17] Delgado-Viscogliosi P., Simonart T., Parent V., Marchand G., Dobbelaere M., Pierlot E., et al. Rapid Method for Enumeration of Viable Legionella pneumophila and Other Legionella spp. in Water. Appl Environ Microbiol 2005;71:4086–96. https://doi.org/10.1128/AEM.71.7.4086–4096.2005.
[18] Wilkinson MG. Flow cytometry as a potential method of measuring bacterial viability in probiotic products: a review. Trends Food Sci Technol 2018;78:1–10. https://doi.org/10.1016/j.tifs.2018.05.006.
[19] Berninger T, González López Ó, Bejarano A, Preininger C, Sessitsch A. Maintenance and assessment of cell viability in formulation of non-sporulating bacterial inoculants. Micro Biotechnol 2018;11:277–301. https://doi.org/10.1111/1751-7915.12880.
[20] Bodor A, Bounedjoum N, Vincze GE, Erdeiné Kis Á, Laczi K, Bende G, et al. Challenges of unculturable bacteria: environmental perspectives. Rev Environ Sci Biotechnol 2020;19:1–22. https://doi.org/10.1007/s11157-020-09522-4.

[21] Hanberger H, Nilsson LE, Nilsson M, Maller R. Post-antibiotic effect of beta-lactam antibiotics on gram-negative bacteria in relation to morphology, initial killing and MIC. Eur J Clin Microbiol Infect Dis 1991;10:927–34. https://doi.org/10.1007/BF02005446.
[22] Maukonen J, Mattila-Sandholm T, Wirtanen G. Metabolic indicators for assessing bacterial viability in hygiene sampling using cells in suspension and swabbed biofilm. LWT - Food Sci Technol 2000;33:225–33. https://doi.org/10.1006/fstl.2000.0650.
[23] Park SY, Kim CG. A comparative study of three different viability tests for chemically or thermally inactivated Escherichia coli. Environ Eng Res 2018;23:282–7. https://doi.org/10.4491/eer.2017.223.
[24] Wang M, Ateia M, Awfa D, Yoshimura C. Regrowth of bacteria after light-based disinfection - what we know and where we go from here. Chemosphere 2021;268:128850. https://doi.org/10.1016/j.chemosphere.2020.128850.
[25] Yura T, Nagai H, Mori H. Regulation of the heat-shock response in bacteria. Annu Rev Microbiol 1993;47:321–50. https://doi.org/10.1146/annurev.mi.47.100193.001541.
[26] Bhunia AK. One day to one hour: how quickly can foodborne pathogens be detected. Future Microbiol 2014;9:935–46. https://doi.org/10.2217/fmb.14.61.
[27] van der Vliet GM, Schepers P, Schukkink RA, van Gemen B, Klatser PR. Assessment of mycobacterial viability by RNA amplification. Antimicrob Agents Chemother 1994;38:1959–65. https://doi.org/10.1128/AAC.38.9.1959.
[28] Diaper JP, Tither K, Edwards C. Rapid assessment of bacterial viability by flow cytometry. Appl Microbiol Biotechnol 1992:38. https://doi.org/10.1007/BF00174481.
[29] Bank HL. Assessment of islet cell viability using fluorescent dyes. Diabetologia 1987:30. https://doi.org/10.1007/BF00275748.
[30] Lu F, Song Y, Huang H, Liu Y, Fu Y, Huang J, et al. Fluorescent carbon dots with tunable negative charges for bio-imaging in bacterial viability assessment. Carbon 2017;120:95–102. https://doi.org/10.1016/j.carbon.2017.05.039.
[31] Boulos L, Prévost M, Barbeau B, Coallier J, Desjardins R. LIVE/DEAD® BacLight™: application of a new rapid staining method for direct enumeration of viable and total bacteria in drinking water. J Microbiol Methods 1999;37:77–86. https://doi.org/10.1016/S0167-7012(99)00048-2.
[32] Schindelin J, Arganda-Carreras I, Frise E, Kaynig V, Longair M, Pietzsch T, et al. Fiji: an open-source platform for biological-image analysis. Nat Methods 2012;9:676–82. https://doi.org/10.1038/nmeth.2019.
[33] Bellali S, Lagier J-C, Raoult D, Bou Khalil J. Among live and dead bacteria, the optimization of sample collection and processing remains essential in recovering gut microbiota components. Front Microbiol 2019;10:1606. https://doi.org/10.3389/fmicb.2019.01606.
[34] Luna LG. Manual of histologic staining methods of the Armed Forces Institute of Pathology. Blakiston Division. McGraw-Hill,; 1968.
[35] Bloom FE, Aghajanian GK. Fine structural and cytochemical analysis of the staining of synaptic junctions with phosphotungstic acid. J Ultrastruct Res 1968;22:361–75. https://doi.org/10.1016/S0022-5320(68)90027-0.
[36] Allan V, Vale R. Movement of membrane tubules along microtubules in vitro: evidence for specialised sites of motor attachment. J Cell Sci 1994;107:1885–97. https://doi.org/10.1242/jcs.107.7.1885.
[37] Forte T.M., Nordhausen R.W. Electron microscopy of negatively stained lipoproteins. Methods in Enzymology, vol. 128, Elsevier; 1986, p. 442–57. https://doi.org/10.1016/0076–6879(86)28086–6.
[38] Acosta-Smith E, Viveros-Jiménez K, Canizalez-Román A, Reyes-Lopez M, Bolscher JGM, Nazmi K, et al. Bovine lactoferrin and lactoferrin-derived peptides inhibit the growth of vibrio cholerae and other vibrio species. Front Microbiol 2018;8:2633. https://doi.org/10.3389/fmicb.2017.02633.
[39] Liu H, Lei M, Du X, Cui P, Zhang S. Identification of a novel antimicrobial peptide from amphioxus Branchiostoma japonicum by in silico and functional analyses. Sci Rep 2015;5:18355. https://doi.org/10.1038/srep18355.
[40] Wang K, Yan J, Chen R, Dang W, Zhang B, Zhang W, et al. Membrane-active action mode of polybia-CP, a novel antimicrobial peptide isolated from the venom of Polybia paulista. Antimicrob Agents Chemother 2012;56:3318–23. https://doi.org/10.1128/AAC.05995-11.
[41] Ni S, Zhou Y, Chen Y, Du X, Zhang S. Identification of ATP synthase α subunit as a new maternal factor capable of protecting zebrafish embryos from bacterial infection. FASEB J 2019;33:12983–3001. https://doi.org/10.1096/fj.201901290R.
[42] Bernard GW, Barkin ME. Cytochemical localization of polysaccharides in bacteria. 983-IN11 Arch Oral Biol 1972;17. https://doi.org/10.1016/0003-9969(72)90121-5.
[43] Cao H, Li C, Qi W, Meng X, Tian R, Qi Y, et al. Synthesis, cytotoxicity and antitumour mechanism investigations of polyoxometalate doped silica nanospheres on breast cancer MCF-7 cells. PLoS ONE 2017;12:e0181018. https://doi.org/10.1371/journal.pone.0181018.
[44] Milojevic T, Albu M, Blazevic A, Gumerova N, Konrad L, Cyran N. Nanoscale Tungsten-Microbial Interface of the Metal Immobilizing Thermoacidophilic Archaeon Metallosphaera sedula Cultivated With Tungsten Polyoxometalate. Front Microbiol 2019;10:1267. https://doi.org/10.3389/fmicb.2019.01267.
[45] Staley JT, Konopka A. Measurement of in situ activities of nonphotosynthetic microorganisms in aquatic and terrestrial habitats. Annu Rev Microbiol 1985;39:321–46. https://doi.org/10.1146/annurev.mi.39.100185.001541.
[46] Bellali S, Lagier J-C, Million M, Anani H, Haddad G, Francis R, et al. Running after ghosts: are dead bacteria the dark matter of the human gut microbiota. Gut Microbes 2021;13:1–12. https://doi.org/10.1080/19490976.2021.1897208.
[47] Lagier J-C, Dubourg G, Million M, Cadoret F, Bilen M, Fenollar F, et al. Culturing the human microbiota and culturomics. Nat Rev Microbiol 2018;16:540–50. https://doi.org/10.1038/s41579-018-0041-0.